



Geochemical Modeling and Quality Assessment of the Surface Waters from the Mouhoun River System, Burkina Faso: Implications of Water–Rock Interactions and Anthropogenic Activities

**Pélagie Wend Bénédoko Korsaga ^a, Aboubakar Sako ^{a,b*}
and Césard Millogo ^{a,b}**

^a *Laboratoire Géosciences et Environnement (LaGE), Département des Sciences de la Terre, Université Joseph Ki-Zerbo, Ouagadougou, Burkina Faso.*

^b *UFR Sciences Appliquées et Technologie, Université Daniel Ouezzin Coulibaly, BP 139, Dédougou, Burkina Faso.*

Authors' contributions

This work was carried out in collaboration among all authors. All authors read and approved the final manuscript.

Article Information

DOI: <https://doi.org/10.9734/irjpac/2024/v25i5876>

Open Peer Review History:

This journal follows the Advanced Open Peer Review policy. Identity of the Reviewers, Editor(s) and additional Reviewers, peer review comments, different versions of the manuscript, comments of the editors, etc are available here: <https://www.sdiarticle5.com/review-history/123500>

Original Research Article

Received: 12/07/2024
Accepted: 14/09/2024
Published: 18/09/2024

*Corresponding author: E-mail: aboubakar.sako@univ-dedougou.bf;

ABSTRACT

Major ion and heavy metal geochemistry was used to investigate the factors that control the Mouhoun River water quality in western Burkina Faso. Major cation concentrations was in the following decreasing order: $\text{Ca}^{2+} > \text{Na}^+ > \text{K}^+ > \text{Mg}^{2+}$, reflecting silicate weathering. However, relatively high HCO_3^- and SO_4^{2-} concentrations could be related to dissolution of calcite and sulfide minerals, respectively. The average heavy metal concentrations in the riverine system were in the following order: $\text{Fe}_T > \text{Ag} > \text{Mn} > \text{Zn} > \text{Pb} > \text{Cu} > \text{Ni} > \text{As}_T > \text{Cr} > \text{Hg} > \text{Co} > \text{Cd}$ with Fe_T and Ag exceeding the World Health Organization permissible limits. Concentrations of all heavy metals, except Cr , were higher in the Mouhoun system compared to the average world river concentrations. Adsorption and speciation models showed that Zn , Ag , Cd , Co , Cr and Ni are likely to remain in their free ionic forms, and thus posing serious threats to aquatic life and human health. Ag-Hg-Ni-Cd association around Poura and Tenado on the principal component plot suggested that the widespread artisanal gold mining in these areas may have contributed to these metals' loading. In contrast, NH_4^+ , Pb , Cu , Cr , As_T and Zn were clustered around a densely populated and industrialized Kou watershed, pointing to agricultural and industrial sources of these pollutants. Furthermore, the Kou River had the highest metal index followed by Tenado, Samendeni, Poura and Boromo. Hence, the chemistry of the Mouhoun River and its tributary appears to be mainly controlled by population density and various anthropogenic activities taking place in their drainage basins. The findings could provide avenues for sound and sustainable water resource management in a water scarce semi-arid environment.

Keywords: Surface water; hydrogeochemistry; major ions; heavy metals; geochemical modeling.

1. INTRODUCTION

The earlier agricultural system that allowed humanity to alter nature and mobilize necessary resources for cultural, scientific and technological progress, was practiced on the banks of the world's largest rivers such as the Huang, the He, the Indus, the Tigris, the Nile and the Euphrates [1,2]. In that sense, rivers are the most important inland water sources for domestic, agricultural and industrial supplies, and thereby play a central role in socio-economic development of many countries around the world. However, the quality of these finite resources, at any given point and time, can be under tremendous pressure from both natural and anthropogenic factors [3,4]. Natural factors such as droughts decrease river water availability and indirectly reduce its quality through competing demands, whereas the quality can be directly affected by flooding and sediment accumulation [5,6,7]. River water quality is also largely affected by the degree of water-rock interactions, soil erosion, dilution/evaporation effects and atmospheric deposition [8,9,10]. Because of their direct contact with various pollution sources and their relative short residence time, river waters are more exposed to point and non-point pollution sources than groundwaters [11].

In order to protect river waters against pollution, the factors that control riverine pollutants'

mobility and toxicity should be properly identified and assessed [12,13]. The hydrogeochemistry and water quality of world's large rivers are a function of several factors such as relief, tectonic and climate settings, underlying geology, soil types, riparian vegetation cover as well as pollution loads from various human activities [14,15]. In the rivers' long course through highly heterogeneous geological formations, these factors may vary considerably making the interpretation of the water quality difficult [16]. In contrast, smaller rivers, such as the Mouhoun River, flow through less diverse geology and climatic zones, and accordingly, the contribution of anthropogenic activities to pollutant loadings can be easily constrained through hydrogeochemical investigations [17]. For instance, quantification of river major ion compositions can reveal the relationships that may exist between, chemical weathering and anthropogenic impacts and the river water quality [18,19,20].

Furthermore, heavy metals, with relatively high densities ($\geq 5 \text{ g/cm}^3$), are among the pollutants that affect most river water quality, as they pose serious threats to human health and ecosystem functioning [21,22,23]. Although these metals can be released into the riverine system through chemical weathering of the underlying and pathway rocks, untreated or partially treated domestic and industrial wastewater and

agricultural runoff, rich in heavy metals, are often discharged into urban and rural riverine systems [24,25,26]. Once in the fluvial system, the heavy metals may be immobilized through precipitation or adsorption. The extent of these geochemical processes depends on pH, mineralogy, redox conditions and the availability of inorganic and organic ligands of the receiving environment [26,27]. Alternatively, the metals could be remained in their ionic forms, and end up in the groundwater system through infiltration [28,29]. Despite their low concentrations in the environment (0.01–100 µg/L), heavy metals distribution in natural waters is of great importance to hydrogeochemical and environmental investigations [30,31]. Some heavy metals (e.g., Fe, Mn, Co, Ni, Cu and Zn) are micronutrients that play an important role in enzyme activities, and can be toxic to biota at high concentrations [32,33], whereas others such as Cd, Pb, As and Hg are highly toxic even at low concentrations [34]. Heavy metals are non-biodegradable, and thus they are potentially toxic with serious ecological and human health ramifications [35]. Consequently, heavy metal environmental contamination is serious global concerns [36,37]. Not only these concerns urge environmental geochemists to thoroughly identify various sources of heavy metals in aquatic system, but also to gain better understanding of the factors that control their behavior and fate.

Several hydrogeochemical methods such as major ion ratios, scatter plots of ion concentrations and multivariate analyses have been traditionally used to study, characterize and evaluate river water quality [38,39,40]. Although these methods are effective in identifying geological controls on water composition and separating anomalous concentrations from natural background concentrations, they cannot adequately predict the behavior and fate of potentially toxic heavy metals in the aquatic systems [41,42,43]. As a result, a series of geochemical modeling such as saturation indices (SI), speciation and adsorption have been widely regarded as crucial for understanding and predicting heavy metal behavior in aquatic environments [44,45].

The Mouhoun River (former Black Volta River) is the largest permanent watercourse in Burkina Faso that flows around several towns including Bobo-Dioulasso, a major urban center and economic hub in the country. To the best of our knowledge, no studies have yet assessed hydrogeochemistry nor evaluated the factors that

control the Mouhoun River water quality for human consumption. In order to reduce this gap of knowledge and provide policymakers with critical information on the river water quality, the main objectives of the present study were to use major ion ratios to highlight the influence of water–rock interaction on the Mouhoun River water, to determine the behavior and fate of selected heavy metals in the water column using R-mode factor analysis and geochemical modeling and to assess the suitability of river water for domestic consumption. Because of the relative short residence time of the flowing water, the extent of anthropogenic activities is likely to be the major factor controlling the Mouhoun River waters. We hypothesize that sampling sites that are located around larger human settlements will have the greatest pollution indices compared to those with smaller settlements.

2. GEOGRAPHICAL AND GEOLOGICAL SETTING

The Mouhoun River basin, with a drainage area of 87,208 km² and total length of about 1,000 km, is part of the large international Volta River Basin [46]. This looped-shape river is fed by numerous springs in southwestern Burkina Faso. The basin is subdivided into three sub-basins namely Sourou (15225 km²), Lower Mouhoun (54802 km²) and Upper Mouhoun (20978 km²) sub-basins. The storage capacity of the reservoirs in the Mouhoun River basin is about 438 million m³ with an average annual filling rate of 65% [47].

The present study was undertaken in the Upper Mouhoun River at Samendeni and in its first major right-bank tributary (Kou River) in southwestern Burkina Faso and in the Lower Mouhoun River in midwestern and central plateau regions (Fig. 1). The Upper Mouhoun River is located in the southeastern edge of the Taoudeni sedimentary basin. This basin consists mainly of dolerites and fine pink and schistose sandstones. The river flows from southwest to northeast, and its basin belongs to Sudanian climatic zone with an average annual rainfall of 1143 mm [48]. Three sampling sites were also selected in the Lower Mouhoun River in Tenado (Midwest region) and Boromo and Poura in the central plateau region. These towns lie within a less wet Sudano-Sahelian climatic zone with an average annual rainfall of about 930 mm. The Lower Mouhoun River drains crystalline basement rocks of Precambrian age associated with the West Africa Craton and composed of a

series of intermediate to basic volcanic rocks and some sandy conglomerates [49]. Two distinct types of savannahs are encountered in the study area namely woodland savannah and grassy savannah [50]. The Upper Mouhoun sub-basin is characterized by densely wooded savannah with tall to medium grasses, whereas grasslands interspersed with trees and shrub is found in the Lower Mouhoun sub-basin.

3. ANTHROPOGENIC SETTINGS

In 2000, the Mouhoun River basin had about 4.5 million inhabitants, and the population is expected to reach 8 million in 2025. The Mouhoun River at Samendeni and the Kou River runs around Bobo-Dioulasso, a city of 904,920 inhabitants [51]. According to the last census in 2006, the populations were 48,694 in Tenado, 14,885 in Boromo and 12,026 in Poura. The urbanization rate was 45,8 % in Samendeni and Kou, 16,4 % in Tenado, 9,6 % in Boromo and Poura in 2019. In addition to domestic water supply, the Mouhoun River water is used for washing, laundry, fishing, irrigation and small-

scale hydropower generation. To meet urban population needs in vegetables and other agricultural products, many people are also involved in urban and peri-urban agriculture in the sampling towns, particularly in Bobo-Dioulasso. Thus, farming takes place in the riparian areas close to the waterbodies along with intensive application of agrochemicals. These activities are likely to be major sources of the river water pollution in the urban area, whereas cotton-growing, uncontrolled cattle grazing and lack of designated watering points for animals pose serious water pollution risks along the Mouhoun River banks in rural areas. Thus, the Mouhoun and Kou rivers are fed by agricultural runoff and domestic and industrial wastewaters of bordering cities and villages. Furthermore, the Mouhoun River basin is exposed to several artisanal gold mining sites, particularly around Tenado and Poura, which could be a major source of water pollution. Construction of dams (e.g., Samendeni and Lery dams) on the Mouhoun River could also cause accumulation of sediments and anthropogenic wastes in the waterbodies [52,53].

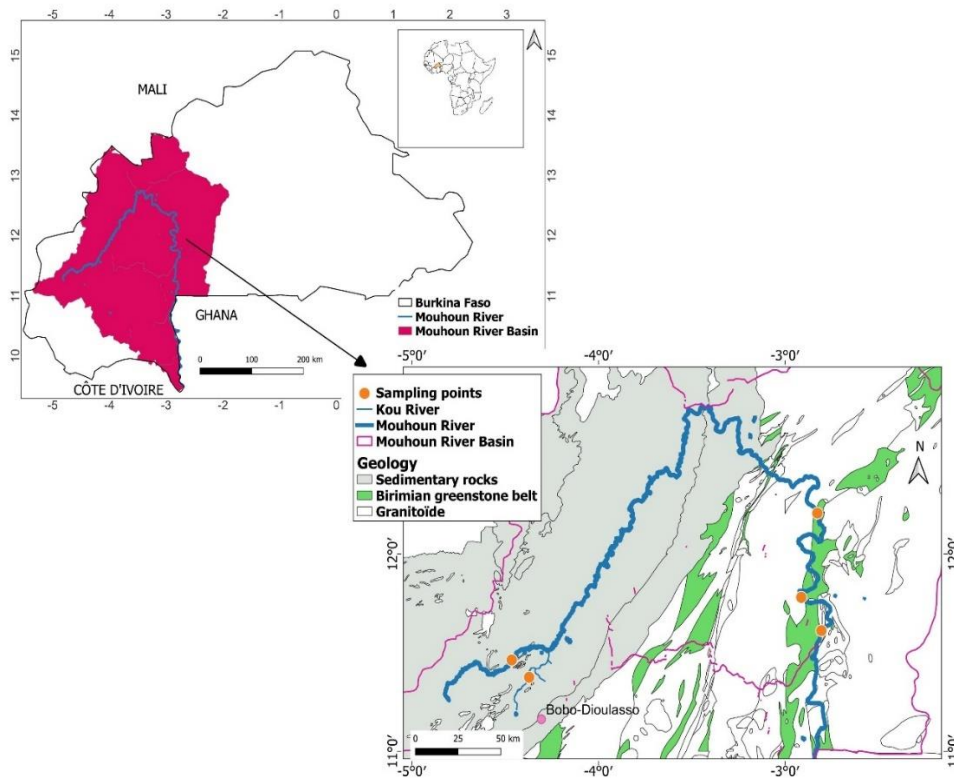


Fig. 1. Localization of the Mouhoun River basin and simplified map of the geology of southwestern Burkina Faso

In Burkina Faso, where a lot of people lack access to clean drinking water and basic sanitation, several management strategies have been undertaken by the Mouhoun River Basin Authority through the Local Water Committees with the objective to reduce pollution loads and sediment transfer from riparian zones to the Mouhoun River system [48]. That is, a 100-m riparian buffer zone has been established around the Mouhoun River across the country. Thus, through a compensation scheme, farmers are encouraged to leave the 100-m zone. As a result, the Local Water Committees play a central role in reducing pollution loads through awareness campaigns about 100-m zone. Despite these efforts, population growth has resulted in larger abstraction of water to meet the increasing demand along with huge volumes of untreated or partially treated domestic and industrial effluents being discharged into the Mouhoun River [54].

4. MATERIALS AND METHODS

4.1 Sampling and Analysis

A suite of 15 surface water samples were collected at three points across the rivers' width in Kou, Samendeni, Tenado, Boromo and Poura using a 1000 mL clean glass immersion sampler during the late wet season 2022 (Fig. 2). These samples are representative of the Mouhoun River and its tributary, the Kou River. pH, electrical conductivity (EC) of the samples were measured *in-situ*, using a calibrated multi-parameter probe. The samples were filtered through 0.45 μm membrane filter and stored in clean unused polyethylene bottles. The filtered water samples were split into two portions. To avoid adsorption of cations onto the container, a portion of water samples was acidified with ultrapure nitric acid to a pH less than 2, and was subsequently used to determine major cation and heavy metal concentrations, whereas major anion concentrations were measured in non-acidified portion.

Back in the laboratory, major cations (i.e., Ca^{2+} , Mg^{2+} , Na^+ and K^+) plus total Fe (Fe_T) and Mn concentrations were determined by Flame Atomic Absorption Spectrophotometer (AAS), whereas those of major anions including Cl^- , SO_4^{2-} , NO_3^- , NO_2^- , PO_4^{3-} and NH_4^+ were measured by UV-visible spectrometer. Bicarbonate concentrations were measured by

titrating samples with 0.1 N HCl and methyl orange indicator. Total hardness (TH) of the samples was determined by EDTA titrimetric technique. A series of heavy metals including Ag, total As (As_T), Cd, Co, Cr, Cu, Hg, Ni, Pb and Zn were analyzed on acidified samples by Inductively Coupled-Mass Spectrometer (ICP-MS). Analytical grad standard stocks were used for the instrument calibration. The detection limits of individual metals for AAS and ICP-MS were calculated using standard deviation of three runs of the blank samples. Concentrations of duplicate and external calibration data of multi-element standards were also used to determine analytical errors, and the results were within 10% error. Instrument calibration and sampling preparation were conducted using ultrapure analytical grad chemicals and Milli-Q water.

In this study, 26 variables were used for multivariate statistical analyses. Concentrations of some ions at certain sampling sites were censored (i.e., concentrations recorded as below the detection limit). Prior to multivariate statistical analyses, all variables (i.e., compositional data), except pH, EC and TH, were centered log-transformed (clr). Hence, one-way analysis of variance (ANOVA) was used to evaluate the differences in the mean of variables of the surface waters at significant values [55,56]. The degree of freedom (df), sum of square (SS) and mean square (MS) between the sampling sites and within sampling sites were determined. Also, F-value (i.e. MS between the clusters/MS within sampling sites) was calculated.

Additionally, R-mode factor analysis with principal component as extraction method was used to investigate the relationships between physico-chemical parameters of the water samples. To obtain stronger component or factor loadings, varimax rotation was applied. Variables loadings are correlation coefficients between the variable and the component. A loading close to ± 1 indicates strong correlation between the variable and the component, whereas a loading close to 0 indicates weak correlation [57,58]. Variables with loadings greater than 0.75 are considered as strongly loaded on a component. In contrast, loadings of 0.4 and 0.5 to 0.75 correspond to weak and moderate loadings, respectively [59]. All statistical analyses were carried out using SPSS statistical software (ver. 23) and OriginPro2022.

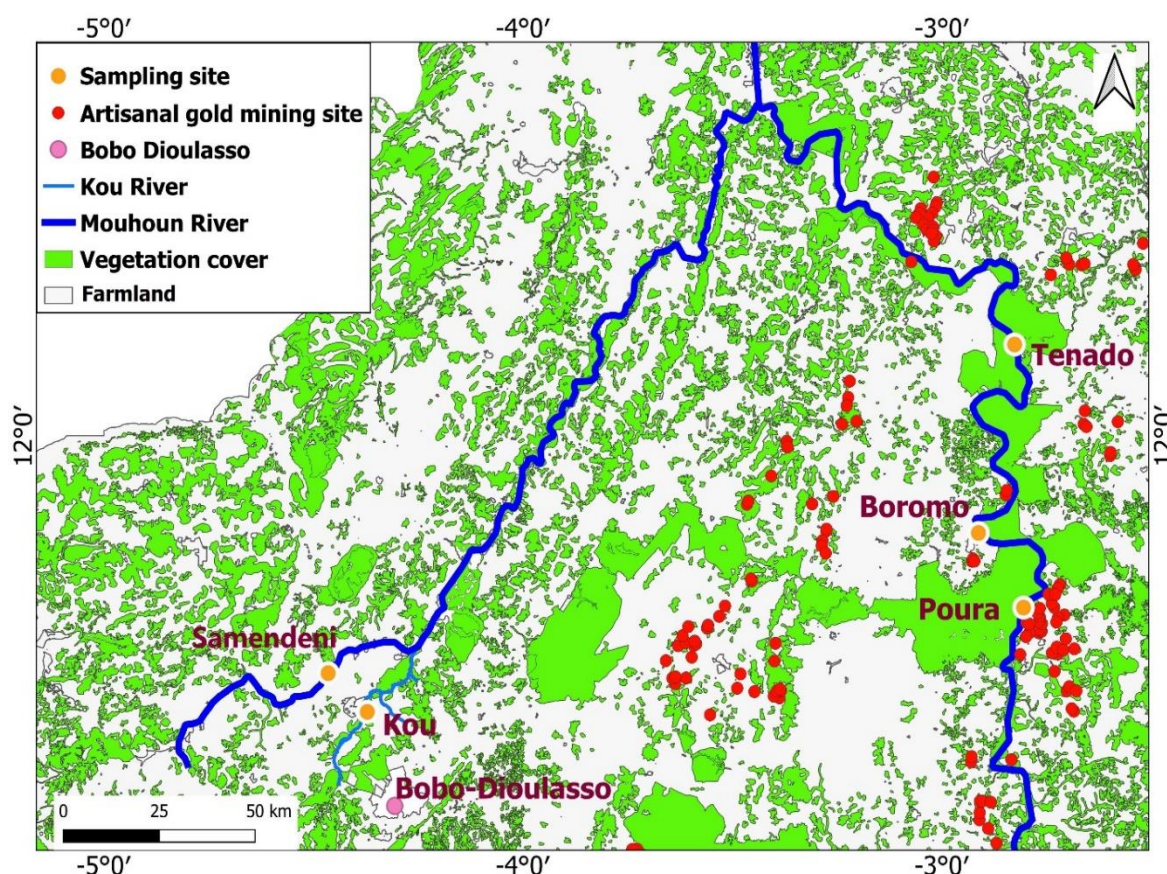


Fig. 2. Map showing the study area and major land use patterns within the Mouhoun River system in Burkina Faso

4.2 Geochemical Modeling

4.2.1 Saturation index

Saturation indices (SI) of a series of mineral phases were used to evaluate the degree of water–rock interactions. Through these indices, geochemical reactions that may control the river water chemistry are identified. These indices were calculated using Visual MINTEQ (Ver. 3.1), a chemical equilibrium code developed by [56], according to the following equation (Eq. 1):

$$SI = \log \frac{IAP}{KT} \quad (1)$$

Where IAP is the logarithm of ion activity product of the dissociated mineral and KT represents the equilibrium constant corrected to the mineral temperature. Visual MINTEQ was also used to calculate partial pressure of CO₂ (pCO₂), activity coefficients by the Davies equation and ionic strength (IS) of the water samples. Likewise, the dominant species of heavy metals were determined in the river water samples.

Average concentrations (mol/L) of hydrous ferric oxide (Fe(OH)₃ and individual heavy metals (i.e., Cd²⁺, Cr²⁺, Cu²⁺, Ni²⁺, Pb²⁺ and Zn²⁺) and ionic strength (IS in mol/L) were used in MINEQL+ a chemical equilibrium modeling system [59,60] to model the metal adsorption onto Fe(OH)₃ at different pH (4.5–8.5). Fitting of the data with Two-Layer model was described by [61]. Densities of strong (0.005 mol/mol Fe) and weak (0.2 mol/mol Fe) binding sites were used, whereas the specific surface area was assumed to be 600 m²/g. The appropriate pH at which heavy metal species are likely to precipitate was also modeled using Hydra-Medusa equilibrium software [62].

4.2.2 Metal index calculation

The metal index (MI) is generally used to evaluate the overall surface and groundwater water quality for drinking and domestic purposes [62-64] and it is defined as (Eq. 2):

$$MI = \sum_{i=1}^n \frac{[M_i]}{(MAC)_i} \quad (2)$$

Where $[Mi]$ is the concentration of each metal and i is the sample, whereas MAC represents the maximum allowable concentration of the metals. Concentrations of 10 heavy metals including Ag, As, Cd, Co, Cr, Cu, Hg, Ni, Pb and Zn were used in the present study to calculate MI. Based on the MI values, the following classes have been used to characterized surface water and groundwater quality [65,66] to very pure ($MI < 0.3$), pure ($0.3 < MI < 1.0$), slightly affected ($1.0 < MI < 2.0$), moderately affected ($2.0 < MI < 4.0$), seriously affected ($4.0 < MI < 6.0$) and strongly affected ($MI > 6.0$).

5. RESULTS AND DISCUSSION

5.1 Major Ion Characteristics

Physico-chemical parameters and major ion concentrations of the Mouhoun River system (main course and tributary) are presented in Table 1. Only pH, EC, TH and Na^+ varied significantly ($p < 0.05$) across the sampling sites (Table 2) with the following decreasing order: (Boromo>Tenado) Tenado>Boromo>Samendeni>Kou>Poura for pH and Poura>Tenado>Boromo>Kou>Samendeni for EC. Similarly, Poura and Tenado showed the highest TH concentrations followed by Boromo, Kou and Samendeni, whereas the highest Na^+ concentrations were found in Boromo and Poura. The relatively low pH, TH and Na^+ concentrations in the Upper Mouhoun River could be attributed to the lithological and vegetation cover differences [67]. The pH values were below the World Health Organization (WHO) recommended values for drinking water and ranged from 6.7 to 7.3 (6.9 ± 0.2), indicating that the river waters were slightly acidic to circumneutral. Likewise, EC, which is an indicator of mineralization of natural waters, were low and varied across the sampling sites ($p = 0.00$) with an average value of $44 \pm 8 \mu S/cm$. The low EC may be attributed to the high velocity of the surface water movement, short residence time and dilution effects during the wet season [68]. This, in turn, has led to lower dissolution, and thereby reducing solute concentrations [69].

With concentrations ranging from 44 to 78 mg/L (67 ± 12 mg/L), HCO_3^- was the dominant major anion in the Mouhoun River system followed by SO_4^{2-} (8.48 ± 0.49 mg/L), Cl^- , NO_3^- , PO_4^{3-} and NO_2^- . The predominance of HCO_3^- in the surface water samples could be related to the dissociation of calcite in the presence of CO_2 [70,71]. Oxidation of organic matter could also

contribute to the high HCO_3^- in surface waters [72]. Although all the major anions had concentrations largely below the WHO recommendation limits for drinking water, the low HCO_3^- (< 100 mg/L) is an indicative of a poor water quality, which is only suitable for industrial activity [73]. In contrast, water with HCO_3^- concentrations comprised between 100 and 250 mg/L are considered having moderate quality and a concentration greater than 250 mg/L correspond to good water quality. Calcium and Na^+ are the most abundant cations, whereas Mg^{2+} had the lowest concentration. The pattern of major cation abundance based on their average concentrations is in following order: $Ca^{2+} > Na^+ > K^+ > Mg^{2+}$, with average concentrations of 8.82 ± 4.3 mg/L, 8.17 ± 7.31 mg/L, 4 ± 0.4 mg/L and 1.2 ± 1.6 mg/L, respectively. The dominance of Ca^{2+} , Na^+ and HCO_3^- in the waters can be explained by weathering of silicate minerals [74,75,76,77]. It can be noticed that average major ion concentrations of the Mouhoun River system are comparable to other world's rivers (Table 1; [78,79]. The low solute contents of the water are also reflected by low TH ($30-70$ mg $CaCO_3/L$ with an average value of 55 ± 11 mg $CaCO_3/L$). With TH less than 70 mg $CaCO_3/L$, the Mouhoun River system is considered as soft [80,81]. Hence, the cationic heavy metals such as Cd, Co, Cr, Cu and Pb are likely to be mobile in the water column.

5.2 Geochemical Processes Controlling Water Chemistry

Interactions between surface water and host rocks is evaluated through several geochemical processes including water composition, chemical weathering, the extents of saturation of the aqueous solution with respect to various mineral phases, ion exchange, oxidation and reduction reactions and adsorption of metals onto secondary minerals [82]. These processes may increase or decrease major ion concentrations or enhance mobility and bioavailability of heavy metals in the aquatic systems [83,84].

In the presence study, the processes controlling the surface water chemistry was described by bivariate mixing plots of Ca^{2+}/Na^+ versus Na^+/Mg^{2+} and Ca^{2+}/Na^+ versus HCO_3^-/Na^+ (Fig. 3a and 3b; [78]. According to the mixing plots, the Mouhoun River samples are clustered around the silicate end member, suggesting that silicate weathering is the dominant water-rock interaction that control the water chemistry. The influence of chemical weathering on the

Mouhoun River water was further evaluated through a series of major ion scatter plots. If halite dissolution was the dominant process of Cl⁻ and Na⁺ abundance in the river waters, the samples would plot along the 1:1 equiline (Fig. 3c). However, it could be noticed that half of the samples are plotted over and below 1:1, respectively. The excess of Na⁺ over Cl⁻ suggesting other sources of Na⁺ such as silicate weathering and ion exchange [85,86,87]. If weathering and dissolution of calcite, dolomite, anhydrite are dominating processes in the water system, the (Ca²⁺+Mg²⁺) versus (HCO₃⁻+SO₄²⁻) scatter plot will be close to the line 1:1 equiline

(Fig. 3d). The silicate weathering can be indicated by the dominance of (HCO₃⁻+SO₄²⁻) over (Ca²⁺+Mg²⁺), whereas the dominance of (Ca²⁺+Mg²⁺) is indicative of reverse ion exchange [86]. In the present study, all samples, except those from Samendeni, showed a dominance of (HCO₃⁻+SO₄²⁻) over (Ca²⁺+Mg²⁺). This is a further indication that silicate weathering was the major lithogenic source of the dissolved ions in the Mouhoun River and its tributary. This was also corroborated by the Piper diagram (Fig. 4), which classified the Mouhoun River as Ca-HCO₃ dominant type, reflecting silicate weathering [88,89].

Table 1. Summary Statistical of physico-chemical parameters and major ion concentrations in water samples from the Mouhoun River system (n = 15)

Parameter	Unit	Min	Max	Mean	SD	Median	World average ¹	WHO (2018)
pH		6.7	7.3	6.9	0.2	6.84	8	7.5-8.5
EC	µs/cm	28	51	44	8	49	–	300
TH	mg CaCO ₃ /L	30	70	55	11	54	–	300
HCO ₃ ⁻	mg/L	44	78	67	12	73	58	120
Cl ⁻	mg/L	<DL	2.6	1.2	0.9	1.7	7.8	250
NO ₃ ⁻	mg/L	0.1	0.51	0.33	0.11	0.3	1	10
NO ₂ ⁻	mg/L	0.03	0.05	0.04	0.01	0.04	–	–
PO ₄ ³⁻	mg/L	0.34	0.41	0.38	0.03	0.4	–	5
SO ₄ ²⁻	mg/L	7.6	9.53	8.48	0.49	8.52	11.2	250
Ca ²⁺	mg/L	8.82	23.65	16.41	4.29	16.83	15	75
Mg ²⁺	mg/L	1.2	6.6	3.3	1.6	3.39	4.1	50
Na ⁺	mg/L	8.17	36.94	17.18	7.31	18.8	6.3	200
K ⁺	mg/L	4	5.52	4.44	0.39	4.395	2.3	12
NH ₄ ⁺	mg/L	0.05	4.08	0.44	1.01	0.18	–	–

¹(Gaillardet et al., 1999; Meybeck, 2003)

Table 2. Analysis of variance of the hydrogeochemical parameters and centered log ratio-transformed (clr) major ion and heavy metal concentrations of the surface waters from the Mouhoun River system

Variable	SS	df	MS	F ratio	p level
pH	0.504	4	0.126	21.365	0.00
EC	984.74	4	246.185	688.951	0.00
TH	1102.4	4	275.6	5.679	0.01
clr.HCO ₃ ⁻	0.22	4	0.055	1.582	0.25
clr.Cl ⁻	10.385	4	2.596	2.442	0.12
clr.NO ₃ ⁻	0.547	4	0.137	1.445	0.29
clr.NO ₂ ⁻	0.6	4	0.15	2.449	0.11
clr.PO ₄ ³⁻	0.317	4	0.079	1.544	0.26
clr.SO ₄ ²⁻	0.513	4	0.128	2.51	0.11
clr.Ca ²⁺	0.215	4	0.054	1.18	0.38
clr.Mg ²⁺	1.219	4	0.305	0.718	0.60
clr.Fe _T	1.838	4	0.46	8.722	0.00
clr.Mn	8.815	4	2.204	30.536	0.00
clr.Na ⁺	1.402	4	0.35	4.119	0.03
clr.K ⁺	9.225	4	2.306	0.982	0.46
clr.NH ₄ ⁺	5.105	4	1.276	1.451	0.29

Variable	SS	df	MS	F ratio	p level
clr.Ag	13.491	4	3.373	1.259	0.35
clr.As _T	17.958	4	4.489	1.789	0.21
clr.Cd	4.801	4	1.2	0.603	0.67
clr.Co	5.689	4	1.422	2.125	0.15
clr.Cr	1.289	4	0.322	0.297	0.87
clr.Cu	9.703	4	2.426	2.268	0.13
clr.Hg	33.225	4	8.306	1.832	0.20
clr.Ni	147.362	4	36.841	1.877	0.19
clr.Pb	8.256	4	2.064	2.569	0.10
clr.Zn	13.697	4	3.424	8.411	0.00

SS = sum of square; df = degree of freedom; MS = mean square.

The saturation index (SI) is a factor that indicates mineral saturation due to water chemistry. If SI is greater than zero it indicates oversaturation of water by a given mineral, whereas values of less than zero suggests undersaturation of the mineral, if the mineral is available, will continue to dissolve until saturation. The SI values of carbonate and evaporate minerals for all samples in the Mouhoun River system were undersaturated, whereas those of Fe-oxyhydroxide minerals were oversaturated, indicating that the same geochemical processes are involved in the water chemistry across the sampling sites (Table 3). Ratios of Ca to Mg can be used to describe calcite and dolomite dissolution in water [90]. A Ca/Mg ratio greater than 1, suggests dissolution of calcite, whereas a value less or equal to 1 indicates dolomite dissolution. In the present study all samples had Ca/Mg > 1 (Fig. 3d), implying that in addition to silicate weathering, dissolution of calcite minerals contributes to the water chemistry.

5.3 Distribution and Geochemical Modeling of River Water

Only three variables (Fe_T, Mn and Zn) differed significantly among the sampling ($p < 0.05$; Table 2). Two variables (Fe_T and Ag) had average concentrations above the WHO's permissible limits for drinking water (Table 4). The average concentrations of the heavy metals were lower than those measured in the mine-impacted Witwatersrand River [91], whereas the average concentrations of As_T, Cd, Cr, Cu, Ni, Pb and Zn were higher in the Rhine River compared to the Mouhoun River system [92]. Only the average concentrations of As_T and Cd in the Mississippi River were higher than those of the Mouhoun River basin system. However, the average concentrations of all metals, except Cr, were higher than the world average river concentrations [93]. The average concentrations of heavy metals in the Mouhoun River system followed the order of Fe_T > Ag > Mn > Zn > Pb > Cu >

Ni > As_T > Cr > Hg > Co > Cd. The relative high concentrations of Fe_T, Mn and Hg in the Mouhoun River system with respect to the world rivers, can be attributed the local geology, pedogenic processes and widespread use of Hg in artisanal gold mining in the areas.

Several geochemical processes such as co-precipitation with metal-oxyhydroxides and adsorption onto the surface of river sediments are likely to control heavy metal distribution and bioavailability in the riverine system [97,98]. Once in the riverine system, behavior and fate of heavy metals will be a function of the environmental conditions such as pH, mineralogy of the drainage basin and oxidation potential [99,100]. Thus, heavy metals may remain in free ionic state in the water column, co-precipitate as secondary minerals or adsorbed onto the surface of the riverine sediments [101]. Speciation modeling showed that over 80% of Zn, Ag, Cd, Co, Cr and Ni remained in their free ionic forms within the river water pH range (Fig. 5a and 5b), more easily assimilated by living organisms [102,103]. Interestingly, the speciation modeling predicted that at pH values of 7.8 and 5.6, Cd²⁺ and Cu²⁺ will form labile CdOH⁺ and CuOH⁺, respectively (Fig. 7). Similarly, complexation of Co²⁺ and Ni²⁺ with OH to form labiles CoOH⁺ and NiOH⁺, will occur at pH 7, whereas formation of solid species of Co(OH)₂ and Cd(OH)₂ likely to occur for Co and Cd at pH 8.2 and Ni (Ni(OH)₂) for Ni at pH 9.8, suggesting that these metals are unlikely to be naturally removed from the water column. In general, cadmium (Cd(II)) precipitates around pH 8 in the form of hydroxides [104], which corresponds with our results. As a result, they pose serious threats to aquatic organisms and human health. Although about 90% of Zn was in the free ionic state (Zn²⁺), zinc adsorption onto Fe-oxyhydroxides occurs at pH 6.2, which is within the river water pH range (6.7–7.3). Formation of zinc solid (Zn(OH)₂) is likely occurred at pH 7.8 (Fig. 7).

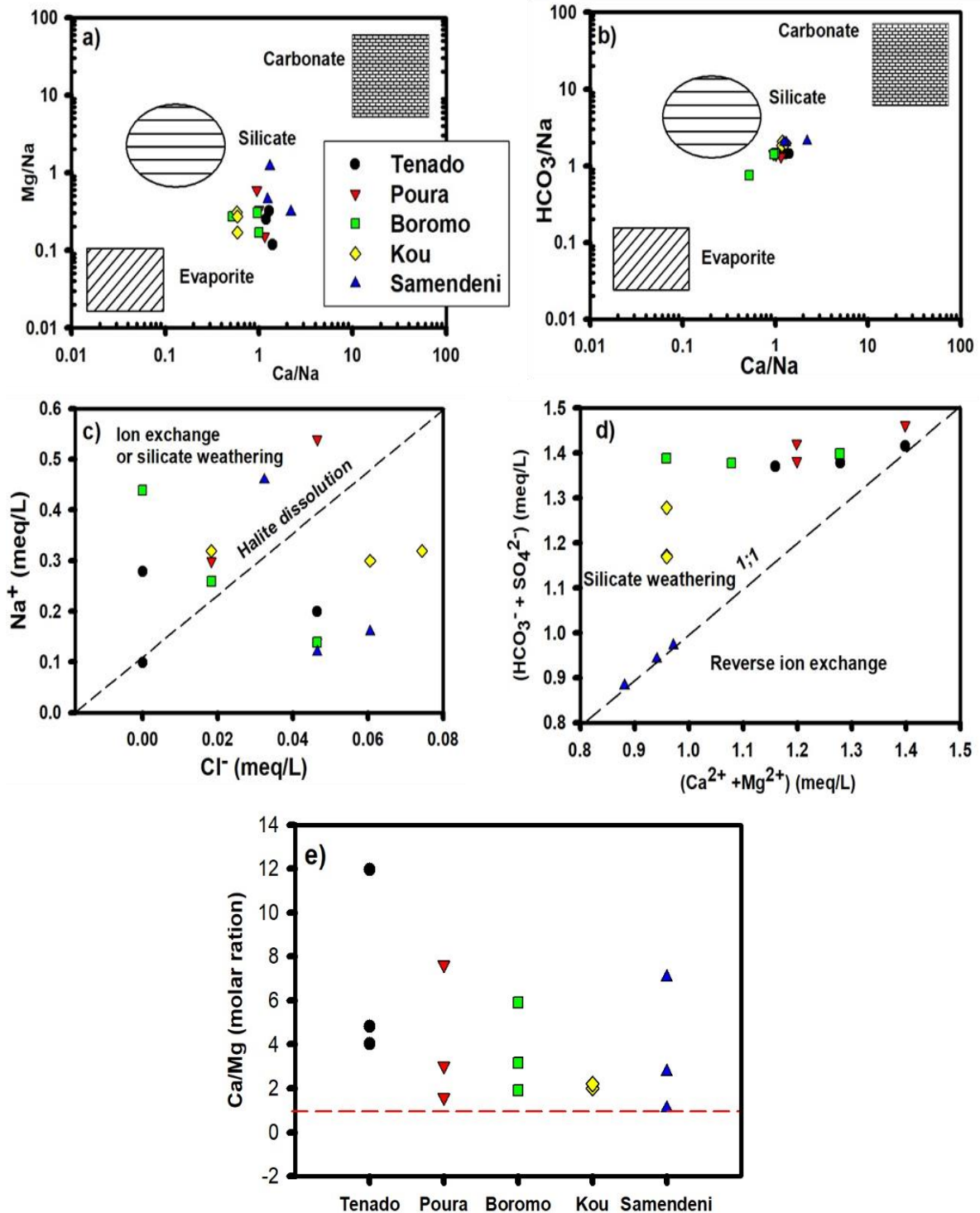


Fig. 3. a-b) Bivariate plots of Na⁺-normalized Ca²⁺ versus Mg²⁺ and Ca²⁺ versus HCO₃⁻ showing evaporite, silicate and carbonate end-members. c-d) Relationships between major ion concentrations, highlighting the main geochemical processes controlling the Mouhoun River system chemistry. e) Scatter plot of molar ratios of Ca/Mg versus sampling sites. The samples with Ca/Mg ratios less than 1 indicate dolomite dissolution, whereas those with ratios greater than 1 correspond to calcite dissolution

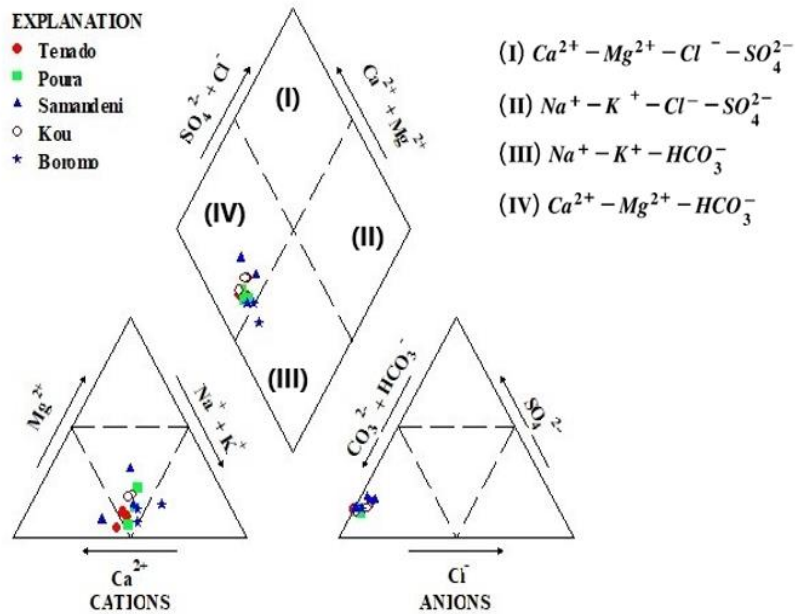


Fig. 4. Piper diagram [88] displaying the dominant water type of the Mouhoun River system
 5.3. Distribution and geochemical modeling of river water

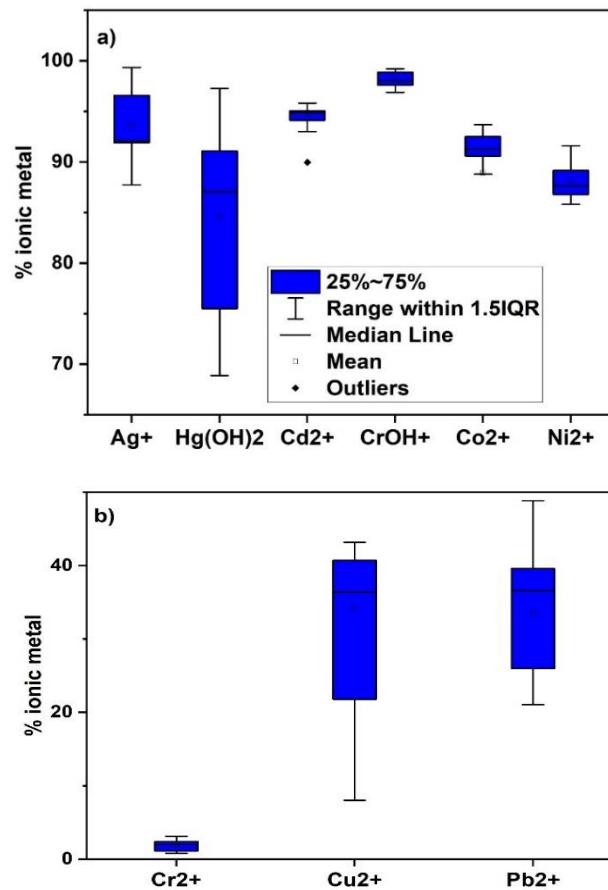


Fig. 5. Proportions of dissolved heavy metal distribution in the Mouhoun River system

Table 3. Saturation indices of mineral phases, ionic strength (IS) and partial pressure (pCO₂) of surface water samples from the River system

Site	Sample	IS (M)	pCO ₂ (atm)	Calcite	Aragonite	Dolomite	Anhydrite	Gypsum	Halite	Cupric Ferrite	Goethite	Ferrihydrite	Hematite
Tenado	T1	0.0024	0.0074	-1.2	-1.4	-3.0	-3.3	-3.0	-3.0	16.0	7.2	4.5	16.7
	T2	0.0025	0.0054	-1.0	-1.1	-2.9	-1.1	-3.0	-10.2	13.4	6.8	4.1	15.9
	T3	0.0027	0.0064	-1.1	-1.2	-2.6	-3.2	-2.9	-10.2	15.8	7.2	4.5	16.9
Poura	P1	0.0025	0.0161	-1.6	-1.7	-3.5	-3.3	-3.0	-9.4	14.1	6.9	4.2	16.3
	P2	0.0027	0.0134	-1.5	-1.6	-3.0	-3.3	-3.0	-9.0	14.1	7.0	4.3	16.4
	P3	0.0025	0.0167	-1.5	-1.7	-3.8	-3.2	-2.9	-9.0	14.4	6.9	4.2	16.2
Samendeni	S1	0.0018	0.0072	-1.6	-1.7	-3.9	-3.3	-3.0	-9.3	13.2	6.9	4.2	16.2
	S2	0.0018	0.0057	-1.8	-1.9	-3.4	-3.5	-3.2	-9.5	13.5	7.0	4.3	16.4
	S3	0.0014	0.0097	-2.1	-2.2	-4.5	-3.6	-3.3	-9.3	14.0	6.7	4.0	15.8
Kou	K1	0.0020	0.0113	-1.6	-1.8	-3.4	-3.5	-3.2	-9.6	15.1	7.3	4.6	17.0
	K2	0.0020	0.0094	-1.6	-1.8	-3.5	-3.4	-3.2	-9.0	14.7	7.3	4.6	17.0
	K3	0.0020	0.0090	-1.6	-1.8	-3.4	-3.4	-3.2	-9.1	15.0	7.3	4.6	17.1
Boromo	B1	0.0022	0.0047	-1.1	-1.2	-2.8	-3.3	-3.0	-9.0	15.4	7.4	4.7	17.2
	B2	0.0023	0.0042	-1.0	-1.2	-2.4	-3.3	-3.1	-9.4	15.9	7.4	4.7	17.1
	B3	0.0030	0.0057	-1.2	-1.3	-2.5	-3.3	-3.0	-9.9	15.7	7.3	4.6	17.0

Table 4. Summary statistical of dissolved trace metal concentrations of the Mouhoun River system (n = 15) compared to other world large rivers as well as to word average river concentrations ($\mu\text{g/L}$)

Trace element	The Mouhoun River					World rivers			World average ^d	WHO (2018)	MAC ^e (2006)
	Min	Max	Mean	SD	Median	Mississippi ^a	Rhine ^b	Witwatersrand ^c			
Fe _T	400	1100	600	200	500	5	35	550000	66	300	300
Mn	24	235	89	75	57	10	5	200000	34	200	50
Ag	0.22	294.20	111.18	81.23	103.40	–	–	–	–	10	100.00
As _T	<DL	4.8	1.5	1.5	1.3	3	13	250	0.62	10	10
Cd	<DL	0.3	0.06	0.09	0	0.1	5.5	52	0.08	20	3
Co	0.1	1.0	0.4	0.3	0.3	–	–	–	0.15	2000	1000
Cr	0.2	4.7	1.2	1.3	0.7	0.5	33	4000	0.7	50	50
Cu	0.1	13.5	2.6	3.3	2	2	34	5400	1.5	10	1000
Hg	<DL	4	1.0	1.4	0.015	0.1	0.65	–	–	6	1
Ni	<DL	15.4	2.4	3.9	1.7	1.5	20	200000	0.8	10	20
Pb	0.8	22.8	8.3	6.5	7.3	0.2	27	6400	0.1	10	10
Zn	<DL	98.3	37.8	38.1	16.3	10	330	26000	0.6	50	5000

^a[94]; ^b[95]; ^c[92]; ^d[93]; ^e[96]

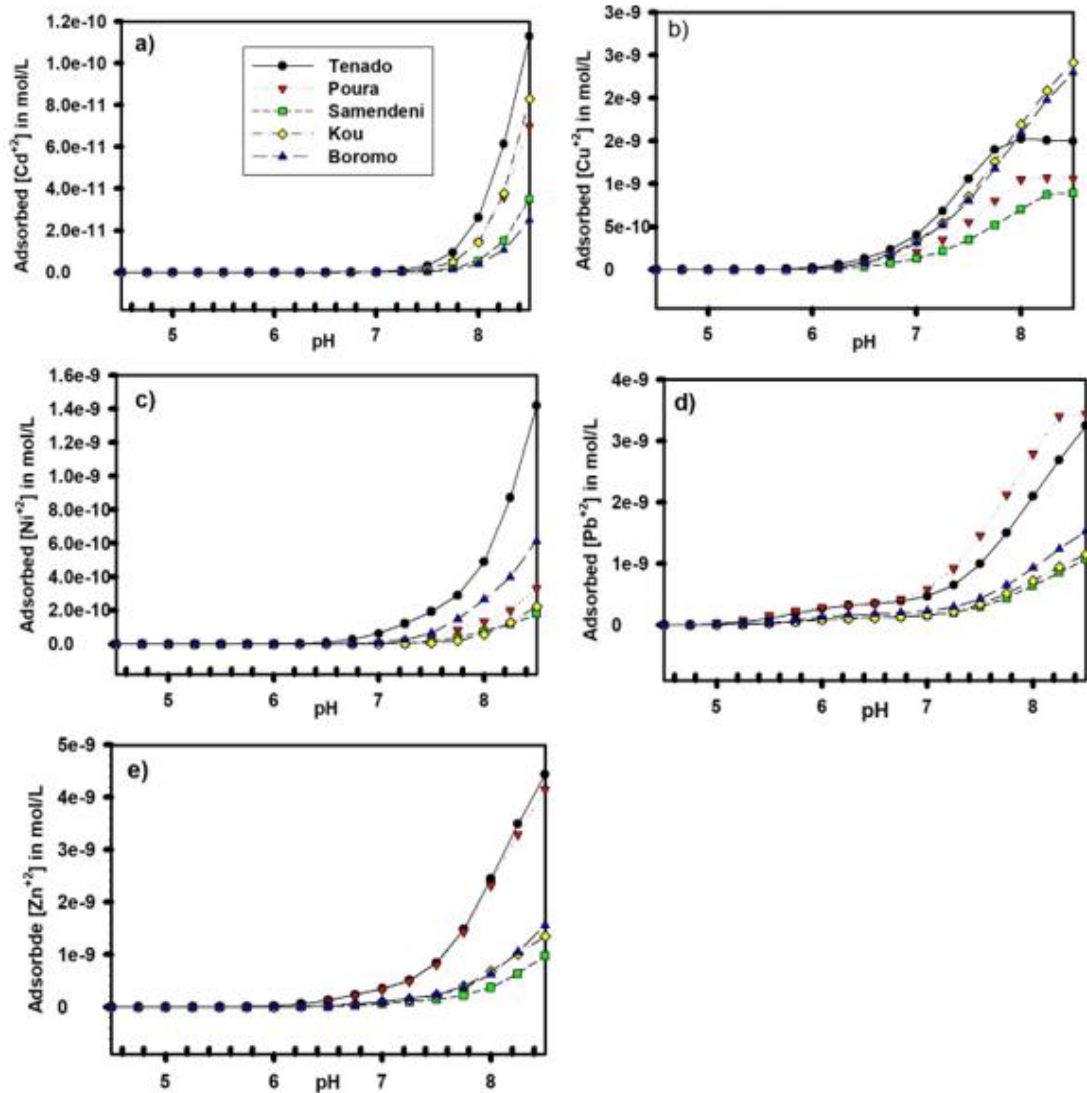


Fig. 6. Expected average heavy metal concentrations adsorbed onto $\text{Fe}(\text{OH})_3$ versus pH in water samples collected in different sites in the Mouhoun River basin

Behavior and fate of Cu and Pb in the riverine system were significantly different from other heavy metals. That is, only about 40% of these metals were in the form of Pb^{2+} and Cu^{2+} in the water column (Fig. 6b). Adsorption of Cu^{2+} and Pb^{2+} onto the Fe-oxyhydroxides started at pH 6.5 and 5.8, respectively. However, occurrence of solid forms of Cr(CrOH)₂, Cu ($\text{Cu}(\text{OH})_2$), Hg ($\text{Hg}(\text{OH})_2$) and Pb (PbOH)₂ is expected at pH 5.4, 7, 2.8 and 8.2, respectively. Adsorption and speciation modeling of heavy metal mobility in the river system was in the following decreasing order: $\text{Ag}^+ > \text{Cd}^{2+} > \text{Ni}^{2+} > \text{Co}^{2+} > \text{Zn}^{2+} > \text{Pb}^{2+} > \text{Cu}^{2+} > \text{Cr}^{2+} > \text{HgOH}^+$. As a result, Ag and Cd may, not only pose serious threats to riparian population, but they may migrate into the groundwater system.

5.4 Anthropogenic Sources of Heavy Metals

To gain insight and understanding of the natural and anthropogenic processes that control distribution of major ions and heavy metals in the Mouhoun River system, R-mode factor was used. After varimax rotation [105], seven principal components (PCs) with eigenvalues greater than unity [106,107] and communalities of the variables close to 1 (Table 5). These components accounted for more than 80% of the total variance, which is reasonably good and can be relied upon to identify the potential sources of the hydrogeochemical parameters of the Mouhoun River system.

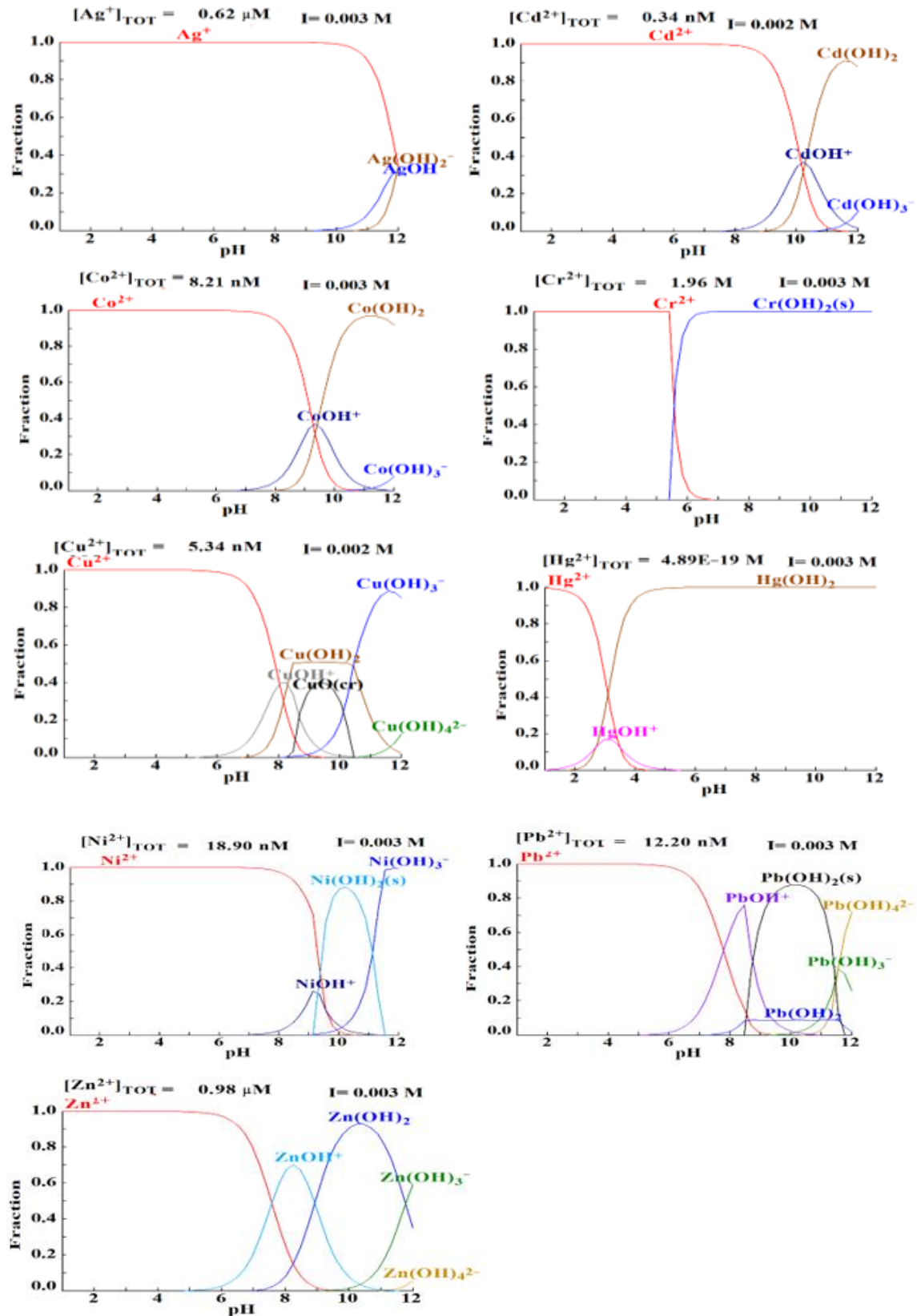


Fig. 7. Expected heavy metal species in the Mouhoun River water as a function of pH

Table 5. R-mode varimax rotated factor analysis loadings (PC-PC7) of hydrogeochemical parameters of the Mouhoun River system

Variable	Component							Communalities
	PC1	PC2	PC3	PC4	PC5	PC6	PC7	
pH	0.03	0.24	-0.15	0.00	0.02	-0.06	0.84	0.789
EC	-0.64	0.38	-0.05	<u>0.45</u>	-0.13	0.24	0.27	0.895
TH	-0.41	0.41	-0.32	<u>0.51</u>	-0.49	-0.12	0.19	0.983
clr.HCO ₃ ⁻	0.46	0.36	<u>0.42</u>	0.37	-0.02	0.39	0.41	0.969
clr.Cl ⁻	0.28	-0.54	0.39	-0.10	0.21	0.03	-0.43	0.762
clr.NO ₃ ⁻	0.10	0.18	0.12	0.85	-0.22	0.08	0.15	0.854
clr.NO ₂ ⁻	0.87	0.17	0.05	-0.18	0.04	0.28	0.05	0.896
clr.PO ₄ ³⁻	0.86	0.00	0.24	0.15	0.01	0.27	0.20	0.935
clr.SO ₄ ²⁻	0.87	0.08	0.29	0.04	0.00	0.28	0.21	0.968
clr.Ca ²⁺	0.18	0.18	-0.06	0.42	-0.22	0.23	0.70	0.834
clr.Mg ²⁺	<u>0.67</u>	0.40	0.32	0.25	-0.16	-0.10	-0.27	0.871
clr.Fe _T	0.26	0.12	0.90	0.10	0.08	-0.09	-0.14	0.928
clr.Mn	0.24	-0.09	0.88	0.00	0.12	-0.06	-0.33	0.966
clr.Na ⁺	0.12	0.69	0.62	-0.42	0.45	0.17	0.09	0.940
clr.K ⁺	-0.09	-0.94	0.08	0.37	-0.09	0.42	0.39	0.975
clr.NH ₄ ⁺	0.20	0.82	0.09	-0.02	-0.04	-0.09	-0.12	0.922
clr.Ag	0.07	-0.95	0.09	-0.11	0.27	0.30	0.18	0.929
clr.As _T	0.05	0.14	-0.10	-0.10	-0.08	0.07	-0.07	0.939
clr.Cd	-0.04	-0.20	<u>0.46</u>	-0.78	-0.13	0.14	-0.02	0.884
clr.Co	0.12	0.14	0.01	0.12	-0.81	0.10	0.09	0.732
clr.Cr	-0.24	-0.10	-0.15	-0.17	-0.03	0.88	0.15	0.874
clr.Cu	<u>-0.59</u>	0.36	0.33	0.04	0.72	0.18	-0.12	0.741
clr.Hg	-0.28	-0.09	-0.12	0.01	0.28	0.27	0.13	0.656
clr.Ni	-0.20	0.30	-0.25	-0.19	-0.17	-0.74	0.15	0.785
clr.Pb	-0.03	0.15	-0.76	0.41	-0.13	-0.19	-0.08	0.923
clr.Zn	0.28	0.24	<u>0.63</u>	-0.14	<u>0.62</u>	0.10	0.23	0.888
% of Variance	17	16.9	15.7	11.0	9.3	9.0	8.9	
Cumulative %	17	34	50	61	70	79	88	

High loadings (≥ 0.75) are bold and moderate loadings ($\geq 0.5 \leq 0.75$) are underlined.

With 17% of the total of the variance, is the most important component among the seven components. Nitrite, PO₄³⁻ and SO₄²⁻ had strong positive loadings on PC1 and Mg²⁺ and HCO₃⁻ had moderate positive loadings on PC1. This component highlights the influence of sulfate of ammonia and phosphate-bearing fertilizers in the river drainage basin [104]. PC2 had high positive loading for NH₄⁺ and strong negative loadings for K⁺ and Ag. Furthermore, Na⁺ and Cl⁻ had moderate positive and negative loadings on PC2, respectively. Such loadings on PC2 represent contribution of sewage or leakage of manure and fertilizers from agricultural activities under subsonic conditions to the riverine system [108]. PC3, which accounts 15.7% of the total variance, had high positive loadings for Fe_T, and Mn and moderate positive loading of Zn, Cd, and HCO₃⁻ representing effects of both water-rock interactions and urban solid wastes on the riverine chemistry. The inverse high loading of Pb on PC3 suggests that Pb was not derived

from the same source as these heavy metals. Such a loading is usually ascribed to vehicular emissions and urban runoff around big agglomerations. With 11% of the total variance, PC4 was mainly dominated by NO₃⁻ and, to a lesser degree, EC, TH, Ca²⁺, and HCO₃⁻. Thus, PC4 could reflect atmospheric deposition and agricultural runoff. Indeed, the anthropogenic origin of NO₃⁻ would be much more related to agricultural fertilizers according to [109]. PC5 explained 9.3% of the total variance and had high positive loading for Cu and moderate loadings for Zn and Na⁺. This component is likely to represent urban and domestic waste loadings into the river system. PC6 had high loading for Cr and a moderate loading for K⁺, whereas Ni was negatively loaded, anthropogenic and natural sources of these elements (Fig. 8a). PC7 was characterized by high positive loadings for pH and Ca²⁺ and moderate loading for HCO₃⁻, representing weathering of limestone and calcium carbonate bearing rocks and ion

exchange processes [110] accompanied by an increase in pH. Further evidence to this end is provided by the high molar ratios of Ca/Mg of the samples. Mercury did not have loading on any principal component.

The loading plot (Fig. 8) of three first PCs shows three grouping of the river hydrochemical parameters associated with the five sampling

sites. That is, NO_3^- , PO_4^{3-} , Ca^{2+} and NO_2^- , representing agricultural runoff were clustered between Samendeni, Poura and Kou. Seven variables including Ag, Hg, K^+ , Ni, Cl⁻, TH and Cd were grounded around highly impacted artisanal gold mining areas of Poura and Tenado, whereas pH, Co, HCO_3^- , Na^+ , Fe_T, EC and Mn, which are dominated by water-rock interactions were associated with Kou, and

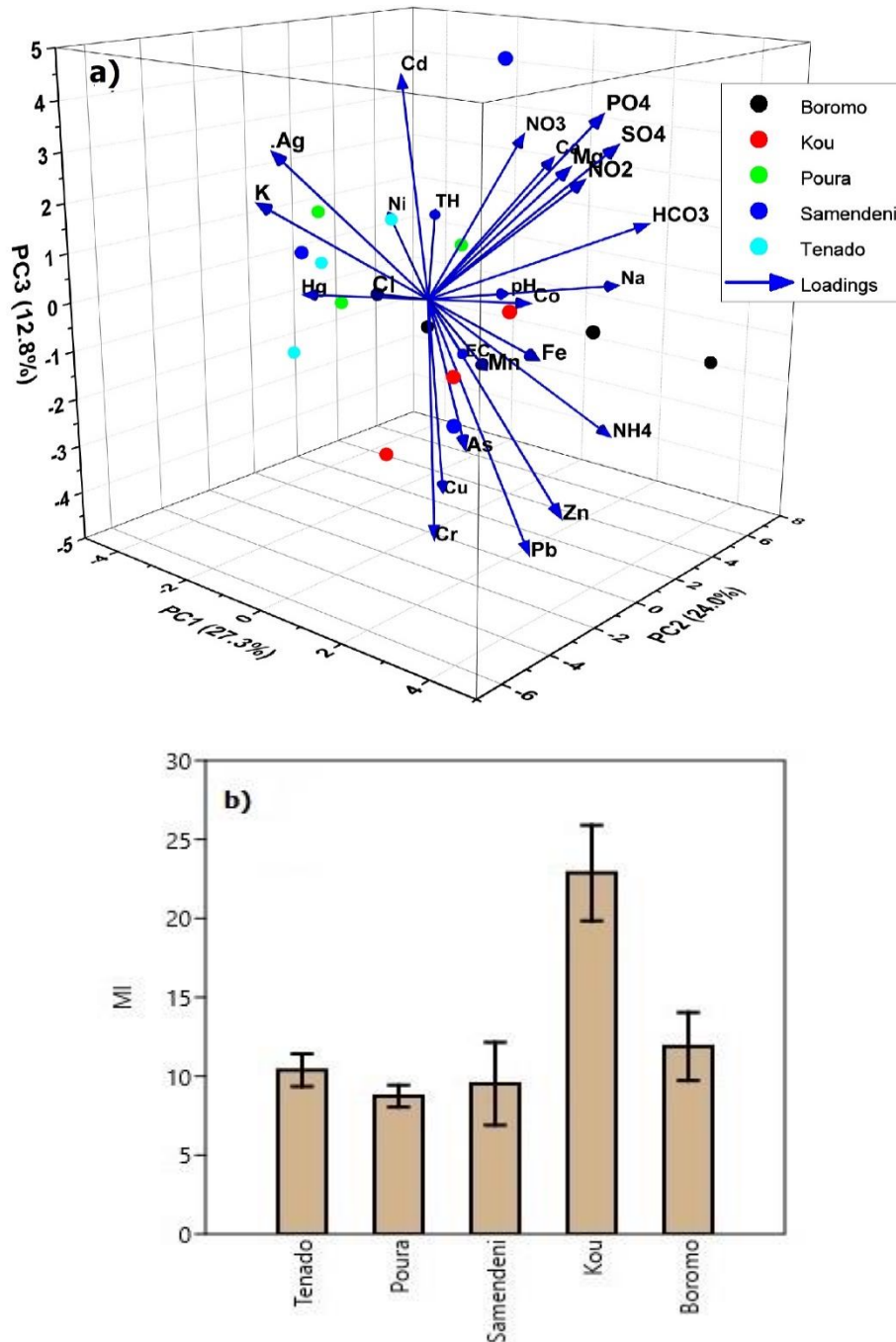


Fig. 8. a) Biplot of two first dominant principal component loadings b) Heavy metal index distribution in different sites

Boromo. Variables that directly related to organic matter decomposition (NH_4^+), vehicular emission (Pb) and industrial wastes (Cu, Cr, As and Zn) were clustered around Kou. The most affected site by anthropogenic activities was identified by using the metal index (MI). The MI values varied broadly from 4 to 15 with an average value of 7 ± 1.6 . Although the Mouhoun River water samples from Boromo had the lowest MI (4.8 ± 1.1), these waters are considered as seriously affected. The highest MI (Fig. 8b) is measured in water samples from the Kou River (11.9 ± 2) followed by Tenado (6.4 ± 1), Samendeni (6.0 ± 2) and Poura (5.7 ± 0.7) from the Mouhoun River. It is noteworthy that the Kou River drains the surface runoff of Bobo-Dioulasso and its surroundings. The study clearly showed a positive correlation between the extents of urbanization and the quality of the surface water from the Mouhoun River system.

6. CONCLUSION

The present study seeks to understand the factors that control the Mouhoun River water quality using a combination of statistical and geochemical modeling. The results of bivariate mixing plots, the major ion ratios and the Piper diagram successfully identified silicate weathering as the major lithogenic source of the dissolved ions in the Mouhoun River and its tributary (Kou River). However, anthropogenic activities such as industrial activities, farming, domestic effluents and artisanal gold mining appeared to enhance heavy metal loading the riverine system. With the highest urbanization level within its drainage basin, the Kou River, is, by far, the most affected by farming and industrial activities, whereas, areas with widespread artisanal gold mining such as Poura and Tenado, are more affected by Hg and Ag. Water samples were oversaturated with respect Fe-oxyhydroxide minerals, suggesting that heavy metals may be co-precipitated with along with these minerals. However, adsorption and speciation modeling showed that all heavy metals, at various degree, are likely to remain in their ionic free species within the pH range of the riverine waters. Further studies including more samples and taking into account the effects of seasonal variations on the Mouhoun River water chemistry are highly recommended.

DISCLAIMER (ARTIFICIAL INTELLIGENCE)

Author(s) hereby declare that NO generative AI technologies such as Large Language Models

(ChatGPT, COPILOT, etc) and text-to-image generators have been used during writing or editing of manuscripts.

ACKNOWLEDGEMENTS

The authors would also like to thank two anonymous reviewers for their helpful comments and suggestions which have greatly improved the early version of the manuscript. This work was supported by the the Higher Education Support Project (PAES). IDA, D357-BF.

COMPETING INTERESTS

Authors have declared that no competing interests exist.

REFERENCES

1. Hassan FA. The dynamic of a riverine civilization: A geoarchaeological perspective on the Nile Valley, Egypt. *World Archaeol.* 1997;29:51–74.
2. Macklin MG, Lewin J. The rivers of civilization. *Quat Sci Rev.* 2015;114: 228244.
3. Khatri N, Tyagi S. Influences of natural and anthropogenic factors on surface and groundwater quality in rural and urban areas. *Front Life Sci.* 2015;8:1:23–39.
4. Akhtar N, Ishak MIS, Bhawani SA, Umar K. Various natural and anthropogenic factors responsible for water quality degradation: a review. *Water.* 2021;13(19):1– 35.
5. Hrdinka T, Novický O, Hanslík E, Rieder M. Possible impacts of floods and droughts on water quality. *J Hydro-Environ Res.* 2012;6(2):145–150.
6. Matys Grygar T, Sedláček J, Bábek O, Nováková T, Strnad L, Mihaljevič M. Regional contamination of Moravia (South-Eastern Czech Republic): temporal shift of Pb and Zn loading in fluvial sediments. *Water Air Soil Pollut.* 2012;223(2), 739–753.
7. Chen J-B, Gaillardet J, Bouchez J, Louvat P, Wang M YN. Anthropophile elements in river sediments: overview from the Seine River, France. *Geochem Geophys Geosyst.* 2014;15(11): 4526– 4546
8. Badruzzaman M, Pinzon J, Oppenheimer J, Jacangelo JG. Sources of nutrients impacting surface waters in Florida: a review. *J Environ Manage.* 2012; 109: 80–92.

9. Lintern A, Webb JA, Ryu D, Liu S, Bende-Michl U, Waters D, Leahy P, Wilson P, Western AW Key factors influencing differences in stream water quality across space. *Rev Water*. 2018; 5 (1) : 1–31.
10. Abdul-Aziz OI, Ahmed S. Evaluating the emergent controls of stream water quality with similitude and dimensionless numbers. *J Hydrol Eng*. 2019; 24 (5) : 1–12.
11. Voutsis N, Kelepertzis E, Tziritis E, Kelepertzis A. Assessing the hydrogeochemistry of groundwaters in ophiolite areas of Euboea Island, Greece, using multivariate statistical methods. *J Geochem Explor*. 2015; 159: 79–92.
12. Lourino-Cabana B, Lesven L, Billon G, Proix N, Recourt P, Ouddane B., Fisher JC, Boughriet, A. Impacts of Metal Contamination in Calcareous Waters of Deûle River (France): Water Quality and Thermodynamic Studies on Metallic Mobility. *Water Air Soil Pollut*. 2010; 206(1-4), 187–201.
13. Jiang L, Yao Z, Liu Z, Wang R, Wu S. Hydrochemistry and its controlling factors of rivers in the source region of the Yangtze River on the Tibetan Plateau. *J Geochem Explor*. 2015; 155:76–83.
14. Chua EM, Wilson SP, Vink S, Flint N (2019) The influence of riparian vegetation on water quality in a mixed land use river basin. *River Res Appl*. 2019; 35: 259–267.
15. Ding X, Liu L. Long-Term Effects of Anthropogenic Factors on Nonpoint Source Pollution in the Upper Reaches of the Yangtze River. *Sustainability*. 2019; 11(8): 1–20.
16. Onderka M, Wrede S, Rodný M, Pfister L, Hoffmann L, Krein A. Hydrogeologic and landscape controls of dissolved inorganic nitrogen (DIN) and dissolved silica (DSi) fluxes in heterogeneous catchments. *J Hydrol*. 2012 ; 450-451: 36–47.
17. Singh VB, Madhav S, Pant NC, Shekhar R (Eds.) (2023) *Weathering and Erosion Processes in the Natural Environment*. John Wiley & Sons.
18. Varol M, Gökot B, Bekleyen A, Şen B. Geochemistry of the Tigris River basin, Turkey. Spatial and seasonal variations of major ion compositions and their controlling factors. *Quat Int*. 2013; 304: 22–32.
19. Gurumurthy GP, Balakrishna K, Tripti M, Audry S, Braun J-J, Lambs L Shankar HNU. Sources of major ions and processes affecting the geochemical and isotopic signatures of subsurface waters along a tropical river, Southwestern India. *Environ Earth Sc*. 2015;i 73: 333–346.
20. Tiwari AK, Singh AK, Giri S, Mahato MK. Major ion chemistry and hydrochemical processes controlling water composition of Teesta River catchment, Sikkim Himalaya, India. *Int J Environ*. 2023 ; 103(20): 8597–8615.
21. Ahmad MK, Islam S, Rahman S, Haque MR, Islam MM. Heavy metals in water, sediment and some fishes of Buriganga River, Bangladesh. *Int J Environ Res*. 2010; 4 (2): 321–332.
22. Li Y, Zhou Q, Ren B, Luo J, Yuan J, Ding X, Bian H, Yao X. Trends and Health Risks of Dissolved Heavy Metal Pollution in Global River and Lake Water from 1970 to 2017. *Reviews of Environmental Contamination and Toxicology*. In: de Voogt, P. (eds) *Reviews of Environmental Contamination and Toxicology Volume 251. Reviews of Environmental Contamination and Toxicology*, vol 251. Springer, Cham. 2019;1–24.
23. Zamora-Ledezma C, Negrete-Bolagay D, Figueroa F, Zamora-Ledezma E, Ni M, Alexis F, Guerrero VH. Heavy metal water pollution: A fresh look about hazards, novel and conventional remediation methods. *Environ Sci Technol*. 2021; 1 – 26.
24. Akpor OB, Muchie M. Environmental and public health implications of wastewater quality. *Afr J Biotechnol*. 2011;10 (3): 2379–2387.
25. Tariq A, Mushtaq A. Untreated Wastewater Reasons and Causes: A Review of Most Affected Areas and Cities. *Int J Chem Biol Sci*. 2023; 23(1): 121–143.
26. Taylor SD, He Y, Hiscock KM. Modelling the impacts of agricultural management practices on river water quality in Eastern England. *J Environ Manag*. 2016; 180: 147–163.
27. Miranda LS, Wijesiri B, Ayoko G A, Egodawatta P, Goonetilleke A. Water-sediment interactions and mobility of heavy metals in aquatic environments. *Water Res*. 2021; 202:1–9.
28. Shahabudin MM, Musa S. Occurrence of Surface Water Contaminations: An Overview. *IOP Conf. Ser. Earth Environ Sci*. 2018; 140:012058.

- DOI 10.1088/1755-1315/140/1/012058.
29. Ganvir PS, Guhey R, Hydro-geochemical elucidation and its implications in the Wardha valley coalfields of central India. In IOP Conference Series: Earth and Environmental Science. 2022;1032(1);012015.
 30. Pasquini AI, Depetris PJ. Hydrochemical considerations and heavy metal variability in the middle Paraná River. *Environ. Earth Sci.* 2012; 65: 525–534.
 31. Zeng J, Han G, Hu M, Wang Y, Liu J, Zhang S, Wang D. Geochemistry of Dissolved Heavy Metals in Upper Reaches of the Three Gorges Reservoir of Yangtze River Watershed during the Flood Season. *Water.* 2021; 13(15):1–15.
 32. Milačić R, Zuliani T, Vidmar J, Oprčkal P, Ščančar J. Potentially toxic elements in water and sediments of the Sava River under extreme flow events. *Sci Total Environ.* 2017; 605-606: 894–905.
 33. Ganvir PS, Papadkar JN, hydro-geochemistry and human health: a brief review. *Int. J. Food Nutrit. Sci.* 2022; 11(11); 223-227.
 34. Aktar MW, Paramasivam MG, anguly M, Purkait S, Sengupta D (2010) Assessment and occurrence of various heavy metals in surface water of Ganga river around Kolkata: a study for toxicity and ecological impact. *Environ Monitor Assess.* 2010; 160 (1– 4): 207–213.
 35. Papadkar JN, Ganvir PS, Nimbarte GR, Patre PP, Barsagade AU and Chandekar RD. A review over the causal relationship between hydro-geochemistry and bioaccumulation in special reference to coalfields. *Eur. Chem Bull* 12(Spl. Iss. 4): 2023;12(4);15288-15297.
 36. Lee CL, Li XD, Zhang G, Li J, Ding AJ, Wang T. Heavy metals and Pb isotopic composition of aerosols in urban and suburban areas of Hong Kong and Guangzhou, South China Evidence of the long-range transport of air contaminants. *Environ Pollut.* 2007; 41 (2) : 432–447.
 37. Lohani MB, Singh S, Rupainwar DC, Dhar DN. Seasonal variations of heavy metal contamination in river Gomti of Lucknow city region. *Environ Monitor Assess.* 2008; 147 (1–3): 253–263.
 38. Garizi AZ, Sheikh V, Sadoddin A. Assessment of seasonal variations of chemical characteristics in surface water using multivariate statistical methods. *Int J Environ Sci Technol.* 2011; 8: 581–592.
 39. Gamble A, Babbar-Sebens M. On the use of multivariate statistical methods for combining in-stream monitoring data and spatial analysis to characterize water quality conditions in the White River Basin, Indiana, USA. *Environ Monit Assess.* 2011; 184(2): 845–875.
 40. Ogwueleka TC. Use of multivariate statistical techniques for the evaluation of temporal and spatial variations in water quality of the Kaduna River, Nigeria. *Environ Monit Assess.* 2015; 187 (137):1 – 17.
 41. Tamma Rao, G., Gurunadha Rao VVS., Srinivasa Rao Y, Ramesh G. Study of hydrogeochemical processes of the groundwater in Ghatprabha river sub-basin, Bagalkot District, Karnataka. India. *Arab J Geosci.* 2012;6:2447–2459.
 42. Güler C, Thyne GD. Delineation of hydrochemical facies distribution in a regional groundwater system by means of fuzzy c-means clustering. *Water Resour Res.* 2004; 40:1 – 11.
 43. Mano JK, Ghosh S, Padhy PK. Characterization and classification of hydrochemistry using multivariate graphical and hydrostatistical techniques. *Res J Chem Sci.* 2013; 3: 32–42.
 44. Namieśnik J, Rabajczyk A. The speciation and physico-chemical forms of metals in surfac waters and sediments. *Chem Speciat Bioav.* 2010; 22(1): 1–24.
 45. Domingos RF, Gélabert A, Carreira S, Cordeiro A, Sivry Y, Benedetti MF. Metals in the Aquatic Environment—Interactions and Implications for the Speciation and Bioavailability: A Critical Overview. *Aquat Geochem.* 2014; 21: 231–257.
 46. Dayinday SA. Assessment and Spatial Analysis of Land Use and Land Cover (LULC) Dynamics in the Black Volta Basin: A Multi-Sensor Remote Sensing and GIS Approach. *Scholar J Sci Tech.* 2023; 4(4):158–177.
 47. François Z, Lucien D, Sarah D. State of Knowledge scientifiques on water resources in Burkina Faso and the impact of climate change on these resources. Scientific Support Project to the National Adaptation Plans National Adaptation Plan. 2019; 58.
 48. Traoré F (2007) Méthodes d'estimation de l'évapotranspiration réelle à l'échelle du

- bassin versant du Kou au Burkina Faso. Université de Liège, Mémoire de DEA en Sciences de Gestion de l'Environnement ; 2007.
49. Hottin G, Ouedraogo OF. Notice explicative de la carte géologique 1/1 000 000 de la République de Haute-Volta: Paris, Bur Recherches Geol Mine. 1975 ; 58.
 50. Siaw D. State of forest genetic resources in Ghana. Sub-regional Workshop AO/IPGRI/ICRAF on the conservation, management, sustainable utilization and enhancement of forest genetic resources in Sahelian and North-Sudanian Africa (Ouagadougou, Burkina Faso, September 22-24, 1998). Forest Genetic Resources Working Papers, Working Paper FGR/17E. Rome, Italy: Food and Agriculture Organization of the United Nations (FAO); 2001.
 51. INSD. Cinquième Recensement Général de la Population et de l'Habitation du Burkina Faso. Synthèse des résultats définitifs ; 2022.
 52. Palanques A, Grinalt J, Betzunces M, Estradas F, Puig P, Guille J. Massive accumulation of highly polluted sedimentary deposits by river damming. *Sci Total Environ.* 2014; 497 498: 369 – 381.
 53. Carr G, Barendreaht MH, Balana BB, Debevec L. Exploring water quality management with a socio-hydrological model: a case study from Burkina Faso. *Hydrolog Sci J.* 2022; 67: 831–846.
 54. Van de Giesen N, Andreini M., van Edig A., Vlek P. Competition for water resources of the Volta Basin. In: Regional management of water resources, proceedings of a symposium held during the sixth IAHS scientific assembly at Maastricht, the Netherlands, July 2001. Wallingford, UK: IAHS Publication. 2001; 268: 199–205.
 55. Cruz MAS, Gonçalves Ad, de Aragão R, de Aragão R, de Amorim JRA, Melo da Mota PV, Srinivasan VS, Garcia CAB, de Figueiredo EE. Spatial and seasonal variability of the water quality characteristics of a river in Northeast Brazil. *Environ Earth Sci.* 2019; 78, 68:1–11.
 56. Pujar PM, Kenchannavar HH, Kulkarni RM, Kulkani UP. Real-time water quality monitoring through Internet of Things and ANOVA-based analysis: a case study on river Krishna. *Appl Water Sci.* 2020;10, 22: 1–16.
 57. Davis JC (1986) *Statistics and data analysis in geology*. 2nd ed. John Wiley and Sons. 1989;656.
 58. Evansa CD, Daviesa, TD, Wigington PJ, Tranter M, Kretser WA. Use of factor analysis to investigate processes controlling the chemical composition of four streams in the Adirondack, New York. *J Hydrol.* 1996;185:297–316.
 59. Gustafsson JP. Visual MINTEQ, versio 2.30: a window version of MINTEQA2, 2004; version 4.0.
 60. Schecher W, McAvoy DC. MINEQL+: A chemical equilibrium modeling system. Version 4.0 for Windows, Environmental Research Software, 1998, Hallowell, Marine.
 61. Dzombak DA, Morel FMM. (1990) Surface complexation modeling: Hydrous ferric oxide. Wiley Interscience. 1996;416.
 62. Puigdomenech I. *Chemical Equilibrium Diagrams*. 2010;14.07.2011.
 63. Tamasi G, Cini R. Heavy metals in drinking waters from Mount Amiata (Tuscany, Italy). Possible risks from arsenic for public health in the Province of Siena. *Sci Total Environ.* 2004; 327: 41– 51
 64. Boateng TK, Opoku F, Akoto O. Heavy metal contamination assessment of groundwater quality: a case study of Oti landfill site, Kumasi. *Appl water Sci.* 2019; 9(2):1–15.
 65. Lyulko I, Ambalova T, Vasiljeva T. To integrated water quality assessment in Latvia. In:
 - a. MTM (monitoring tailor-made) III, proceedings of international workshop on information for sustainable water management, Netherlands. 2001;449–452.
 66. Mambenga PVI, Maqsoud A, Plante B, Benzaazoua M, Ducharme Y. Physicochemical quality of surface water: Background study prior of the Milky river sub-basin, Abitibi, Canada. *WSEAS Trans Environ Dev.* 2017;13:43–48.
 67. Liu B, Luo J, Jiang S, Wang Y, Li Y, Zhang X., Zhou S. Geochemical fractionation, bioavailability, and potential risk of heavy metals in sediments of the largest influent river into Chaohu Lake, China. *Environ Pollut.* 2021;290: 1–11.
 68. Makhoukh M, Sbaa M, Berrahou A, Clooster MV. Contribution à l'étude

- physico-chimique des eaux superficielles de l'Oued Moulaya (Maroc Oriental). Larhyss J. 2011;9:149–169.
69. Corwin DL, Yemoto K. Salinity: Electrical conductivity and total dissolved solids. Methods of analysis. Soil Sci Soc Am. 2017;J2:1–16.
 70. Sulpis O, Lix C, Mucci A, Boudreau BP. Calcite dissolution kinetics at the sediment-water interface in natural seawater. Mar Chem. 2017;195:70–83.
 71. Thi Bao Le T, Divine-Ayela C, Striolo A., Cole DR. Effects of surface contamination on the interfacial properties of CO₂/water/calcite systems. Phys Chem Phys. 2021;23(34):1 – 8.
 72. Huq ME, Fahad S, Shao ZF, Sarven MS, Al-Huqail AA, Siddiqui MH, Rahman MHU, Khan IA, Alam M, Saeed M, Rauf A, Basir A, Jamal Y, Khan SU. High arsenic contamination and presence of other trace metals in drinking water of Kushtia district, Bangladesh. J Environ Manag. 2019;242: 199–209.
 73. WHO. Guidelines for drinking water quality. World Health Organization, Geneva; 2006.
 74. Gurumurthy GP, Balakrishna K, Riotte J, Braun J-J, Audry S, Shankar HNU, Manjunatha B R. Controls on intense silicate weathering in a tropical river, southwestern India Chem Geol. 2012; 300–301:61–69.
 75. Fan BL, Zhao ZQ, Tao FX, Liu J, Tao Z-H, Gao S, Zhang LH. Characteristics of carbonate, evaporite and silicate weathering in Huanghe River basin: A comparison among the upstream, midstream and downstream. J Asian Earth Sci. 2014; 96: 17–26.
 76. Amrith N, Arun K, Nishitha D, Balakrishna K, Udayashankar, HN, Khare N. Major ion chemistry and silicate weathering rate of a small Western Ghats river, Sharavati, southwestern India. Appl Geochem. 2021; 136: 105182.
 77. Maharana C, Gautam SK, Singh AK, Tripathi JK. Major ion chemistry of the Son River, India: Weathering processes, dissolved fluxes and water quality assessment. J Earth Syst Sci. 2015; 124: 293–1309.
 78. Gaillardet J, Dupré B, Louvat P, Allègre CJ. Global silicate weathering and CO₂ consumption rates deduced from the chemistry of large rivers. Chem Geol, 1999; 159: 3–30.
 79. Meybeck M. Global occurrence of major elements in rivers. Treatise Geochem. 2003; 5: 207–223.
 80. Li PY, Qian H, Wu JH. Hydrochemical Characteristics and Evolution Laws of Drinking Groundwater in Pengyang County, Ningxia, Northwest China. E-J Chem. 2011; 8(2): 565–575.
 81. Li P, Wu J, Qian H. Hydrogeochemistry and Quality Assessment of Shallow Groundwater in the Southern Part of the Yellow River Alluvial Plain (Zhongwei Section), Northwest China. Eart Sci Res. 2014; J 18: 27–38.
 82. Candeias C, Ávila PF, da Silva EF et al. Water–Rock Interaction and Geochemical Processes in Surface Waters Influenced by Tailings Impoundments: Impact and Threats to the Ecosystems and Human Health in Rural Communities (Panasqueira Mine, Central Portugal). Water Air Soil Pollut. 2015;226:23. Available:<https://doi.org/10.1007/s11270-014-2255-8>.
 83. Liu X, Zhou Z, Ding Y. Vegetation coverage change and erosion types impacts on the water chemistry in western China. Sci Total Environ. 2021; 772: 1–12.
 84. Meng L, Zhao L, Liu W, Lian J, Chao L. (2021) Risk assessment of bioavailable heavy metals in the water and sediments in the Yongding New River, North China. Environ Monit Assess. 2012; 193 (9): 1–16.
 85. Gupta H, Chakrapani GJ, Selvaraj K, Kao S-J. The fluvial geochemistry, contributions of silicate, carbonate and saline–alkaline components to chemical weathering flux and controlling parameters: Narmada River (Deccan Traps), India. Geochim Cosmochim Acta. 2011; 75(3): 800–824.
 86. Zhu B, Yu J, Qin X, Rioual P, Zhang Y, Liu Z, Mu Y, Li H, Ren X, Xiong H. Identification of rock weathering and environmental control in arid catchments (northern Xinjiang) of Central Asia. J Asian Earth Sci. 2013; 66277–294.
 87. Tsering T, Abdel Wahed MSM, Iftekhhar S, Sillanpää M. Major ion chemistry of the Teesta River in Sikkim Himalaya, India: Chemical weathering and assessment of water quality. J Hydrol Reg Stud. 2019; 24:1–13.
 88. Elango L, Kannam R. Chapter 11 Rock–water interaction and its control on chemical composition of groundwater.

- Developments in Environmental Science. 2007;(5):229-243.
89. Roy SK, Zahid A. Assessment of river water–groundwater–seawater interactions in the coastal delta of Bangladesh based on hydrochemistry and salinity distribution. *SN Appl Sci.* 2021; 3(4):1 – 20.
 90. Wang M, Yang L, Li J, Liang Q. Hydrochemical Characteristics and Controlling Factors of Surface Water in Upper Nujiang River, Qinghai-Tibet Plateau. *Minerals.* 2022;12: 1–15.
 91. Jalali M. Assessment of the chemical components of Famenin groundwater, western Iran. *Environ Geochem Health.* 2007;29 (5): 357–374.
 92. Piper AM. A graphical procedure in the chemical interpretation of groundwater analysis. *Trans Am Geo Union.* 1944;25: 914– 928.
 93. Wittmann GTW, Förstner U. Metal enrichment of sediments in inland waters - the Jukskei and Hennops River drainage systems. *Water.* 1976; 2: 67–72.
 94. Viers J, Dupré B, Gaillardet J. Chemical composition of suspended sediments in world Rivers: New insights from a new database. *Sci Total Environ.* 2008; 407: 853–868.
 95. Trefry JH, Presley BJ. Heavy metal transport from the Mississippi River to the Gulf of Mexico. In: Windom HL, Duce RA (eds) *Marine pollution transfer.* Heath & Co Lexington. 1976; 39–76.
 96. Heinrichs H. Die Untersuchung von Gesteinen und Gewässern auf Cd, Sb, Hg, Tl, Pb, und Bi mit der flammenlosen Atomabsorptions-Spektralphotometrie. Thesis Univ Gottingen. 1975; 82 pp
 97. MAC. Comité fédéral-provincialterritorial sur l'eau potable. De la source au robinet : Guide d'application de l'approche à barrières multiples pour de l'eau potable saine. Winnipeg : Conseil canadien des ministres de l'environnement ; 2006.
 98. Shi M, Min X, Ke Y, Lin Z, Yang Z, Wang S, Peng N, Yan X, Luo S, Wu J, Wei Y. Recent progress in understanding the mechanism of heavy metals retention by iron (oxyhydr)oxides. *Sci Total Environ.* 2020;752: 1–19.
 99. Li J, Zhao Z, Song Y, You Y, Li J, Cheng X. Synthesis of Mg(II) doped ferrihydrite-humic acid coprecipitation and its Pb(II)/Cd(II) ion sorption mechanism. *Chin Chem Lett.* 2021; 32(10),3231–3236.
 100. Hassimi H, Taleb A, Bouezmarni M, Karzazi O, Taleb M, Kherbeche A, Debbaut V. The effect of the physicochemical conditions variations on the behavior of heavy metals trapped in polluted fluvial system sediments: the case of Oued Sebou, Morocco. *Appl Water Sci.* 2019;(9)17: 1–8.
 101. Deng H, Tu Y, Wang H, Wang Z, Li Y, Chai L, Zhang W, Lin Z. Environmental behavior, human health effect, and pollution control of heavy metal (loid)s toward full life cycle processes. *Eco-Environ Health J.* 2022;1 (4): 229–243.
 102. Rigaud S, Radakovitch O, Couture RM, Deflandre B, Cossa D, Garnier C, Garnier JM. Mobility and fluxes of trace elements and nutrients at the sediment-water interface of a lagoon under contrasting water column oxygenation conditions. *Appl Geochem.* 2013;31: 35–51.
 103. Tang W, Shan B, Zhang H, Zhu X, Li S. Heavy metal speciation, risk, and bioavailability in the sediments of rivers with different pollution sources and intensity. *Environ Sci Pollut Res.* 2016; 23(23): 23630–23637.
 104. Zhang C, Shan B, Tang W, Dong L, Zhang W, Yuansheng Pei Y (2017) Heavy metal concentrations and speciation in riverine sediments and the risks posed in three urban belts in the Haihe Basin. *Ecotoxicol Environ Saf.* 2017; 139: 263–271,
 105. Massart DL, Vandeginste BGM, Deming SN, Michotte Y, Kaufman L. *Chemometrics: A textbook.* Amsterdam: Elsevier. 1988;500.
 106. Kaiser HF. The application of electronic computers to factor analysis. *Educ. Psychol. Measur.* 1960;20:141–151.
 107. Sunkari ED, Abu M. Hydrochemistry with special reference to fluoride contamination in groundwater of the Bongo district, Upper East Region, Ghana. *Sust Water Manag.* 2019;5: 1803–1814.
 108. Singh B, Craswell, E (2021) Fertilizers and nitrate pollution of surface and ground water: an increasingly pervasive global problem. *SN Appl Sci.* 2021;(3) 518:1–24.
 109. Mahamane AA, Guel B. Caractérisations physico-chimiques des eaux souterraines de la localité de Yamtenga (Burkina Faso). *Int J Biol Chem Sci.* 2015; 9(1): 517-533.

110. Okiongbo KS, Douglas RK. Evaluation of major factors influencing the geochemistry of groundwater using graphical and multivariate statistical methods in Yenagoa city, Southern Nigeria. Appl Water Sci. 2015;5(1):27– 37.

Disclaimer/Publisher's Note: The statements, opinions and data contained in all publications are solely those of the individual author(s) and contributor(s) and not of the publisher and/or the editor(s). This publisher and/or the editor(s) disclaim responsibility for any injury to people or property resulting from any ideas, methods, instructions or products referred to in the content.

© Copyright (2024): Author(s). The licensee is the journal publisher. This is an Open Access article distributed under the terms of the Creative Commons Attribution License (<http://creativecommons.org/licenses/by/4.0>), which permits unrestricted use, distribution, and reproduction in any medium, provided the original work is properly cited.

Peer-review history:

The peer review history for this paper can be accessed here:

<https://www.sdiarticle5.com/review-history/123500>